The assumption in the Weiner et al. force fields[13,14] has been that the use of a constant dielectric $\epsilon = 1$ is appropriate with full inclusion of solvent, and that a distance-dependent dielectric $\epsilon = r_{ij}$ is appropriate for implicitly mimicking solvent effects, with no other required changes in the parameters. Obviously, the use of $\epsilon = r_{ij}$ is a very rough approximation used to modulate long-range electrostatic interactions. But it appears to be a reasonable one, since local hydrogen-bonding effects are shown to be similar with both models. In our opinion, it is not appropriate or necessary to derive different force fields in different solvent conditions, as long as one (A) parametrizes to fit experimental data in a given solvent condition by carrying out the calibration free energy calculations in that solvent, and (B) represents the environmental effects with the reasonable accuracy allowed by commonly used liquid solvent models.

In total, it is clear that the choice of force fields model is an important one for quantitative work, and that as the focus of modeling work continues to become more quantitative, we must develop better, and better characterized, force fields by using tools such as those presented here.

Acknowledgment. We thank the NSF (DMB-87-14775) and the San Diego Supercomputing Center for supercomputing time. We also thank the NIH, the National Cancer Institute (CA-25644), and Merck Sharp and Dohme for research support. Finally, we thank reviewer one, whose detailed comments on an alternative philosophy of force field development led us to expand our discussion.

Registry No. Adenosine, 58-61-7; deoxyadenosine, 958-09-8.

π-Stacking and the Platinum-Catalyzed Asymmetric Hydroformylation Reaction: A Molecular Modeling Study

L. A. Castonguay,[†] A. K. Rappé,*[,†] and C. J. Casewit[‡]

Contribution from the Department of Chemistry, Colorado State University, Fort Collins, Colorado 80523, and Calleo Scientific Software Publishers, 1300 Miramont Drive, Fort Collins, Colorado 80524. *Received February 22, 1991*

Abstract: The importance of steric factors in determining the regioselectivity of a class of platinum(II) hydroformylation catalysts ($L_2Pt(CO)X$) has been theoretically examined by using an augmented Dreiding force field. This paper characterizes the differential stabilization of the initially formed platinum alkyl complexes resulting from styrene insertion into a Pt-H bond to form either the primary phenethyl product (leading to normal or linear aldehyde) or the secondary α-methyl styryl intermediate (leading to branched aldehyde). The α-methyl styryl products displayed a pronounced π-stacking interaction between the aryl ligand and an aromatic ring of the phosphine ligand, whereas this interaction was absent in the phenethyl intermediate. When pentene is substituted for styrene, the normal intermediate is favored over the branched intermediate.

Introduction

The hydroformylation reaction or Oxo process produces aldehydes from the reaction of alkenes with synthesis gas ($CO + H_2$). The process was first discovered for a cobalt catalyst,[1] though all group 8, 9, and 10 transition metals show catalytic activity.[1,2] Catalytic asymmetric hydroformylation reactions have been used for the synthesis of optically pure organic products using rhodium and platinum catalysts with optically active ligands.[3,4,5]

Platinum complexes have not been used extensively in asymmetric hydroformylation due to the generally lower reaction rates in comparison with rhodium catalysts, and the tendency for the substrate olefin to undergo competitive hydrogenation.[1] In addition, relatively low branched to normal ratios (b/n ratio) have been observed in the hydroformylation of monosubstituted olefins. Recent work,[3] however, on $L_2PtCl_2/SnCl_2$ catalyst precursors and preformed $L_2PtClSnCl_3$ reports enantiomeric excesses at nearly an acceptable level ($\sim$80% ee). Modest increases in the obtained enantiomeric excess and increased regioselectivity would establish this reaction as being viable for asymmetric synthesis.

Successful asymmetric hydroformylation of olefins requires the control of regiochemistry (b/n ratio) as well as control of absolute stereochemistry (ee) of the branched product. Experimental investigations of asymmetric hydroformylation have focused on developing an understanding of the chiral induction step; factors affecting the regioselectivity have rarely been studied for asymmetric catalysis, and are the focus of the present work.

The intermediacy of a platinum alkyl complex in the Pt(II)-catalyzed hydroformylation reaction has been established by Scrivanti and co-workers.[6] The alkyl is formed from the insertion of an olefin into a Pt-H bond. Olefin insertion/β-elimination reaction pairs are in general reversible,[1] establishing the pair of competing equilibria prior to the rate-limiting steps of each pathway, as shown in eq 1 for a Pt complex.

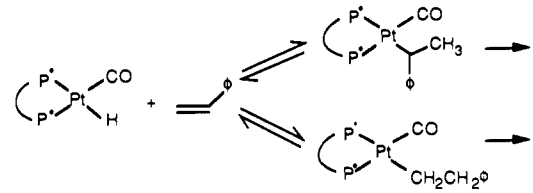

(1)

In the case of asymmetric olefin hydrogenation, those factors favoring the major isomer in the set of equilibria prior to the rate-determining step ultimately adversely affect the rate-deter-

[†] Colorado State University.
[‡] Calleo Scientific Software Publishers.

(1) Parshall, G. W. *Homogeneous Catalysis: The Applications and Chemistry of Catalysis by Soluble Transition Metal Complexes*; Wiley: New York, 1980. Collman, J. P.; Hegedus, L. S.; Norton, J. R.; Finke, R. G. *Principles and Applications of Organotransition Metal Chemistry*; University Science Books: Mill Valley, CA, 1987.

(2) Pruett, R. L. *Adv. Organomet. Chem.* **1979**, *17*, 1-60. Gates, B. C.; Katzer, J. R.; Schuit, G. C. A. *Chemistry of Catalytic Processes*; McGraw-Hill: New York, 1979. Pines, H. *The Chemistry of Catalytic Hydrocarbon Conversions*; Academic Press: New York, 1981.

(3) Stille, J. K.; Parrinello, G. *J. Mol. Catal.* **1983**, *21*, 203. Parrinello, G.; Deschenaux, R.; Stille, J. K. *J. Org. Chem.* **1986**, *51*, 4189. Parrinello, G.; Stille, J. K. *J. Am. Chem. Soc.* **1987**, *109*, 7122. Stille, J. K.; Su, H.; Brechot, P.; Parrinello, G.; Hegedus, L. S. *Organometallics* **1991**, *10*, 1183.

(4) Consiglio, G.; Pino, P. *Top. Curr. Chem.* **1982**, *105*, 77-123. Consiglio, G.; Morandini, R.; Scalone, M.; Pino, P. *J. Organomet. Chem.* **1985**, *279*, 193.

(5) Kawabata, V.; Suzuki, T. M.; Ogata, I. *Chem. Lett.* **1978**, 361.

(6) Scrivanti, A.; Paganelli, S.; Matteoli, U.; Botteghi, C. *J. Organomet. Chem.* **1990**, *385*, 439 and references therein.

0002-7863/91/1513-7177$02.50/0

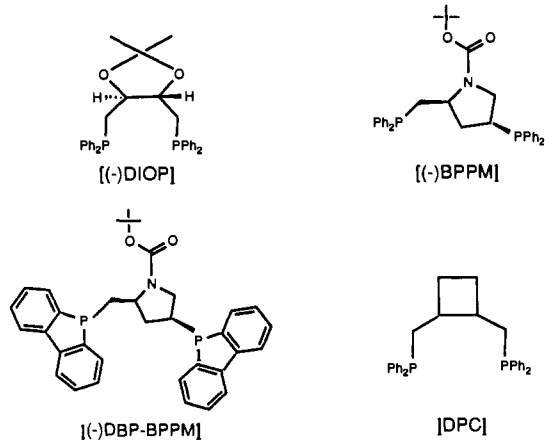

Figure 1. Phosphine ligands.

mining step.[7] This may not be the case for hydroformylation; in fact, we suggest that the direction of insertion of the alkene into the metal hydride bond does contribute to the b/n ratio of aldehydes produced.

As a first step in the theoretical characterization of the importance of steric factors in determining the regioselectivity of a class of platinum(II) hydroformylation catalysts ($L_2Pt(CO)X$), we have augmented the Dreiding force field[8] to include square-planar platinum(II) and a phosphorus capable of binding to transition metals. This force field has been benchmarked on 12 phosphorus Pt(II) acyl and alkyl complexes. The force field has been used to examine the differential stabilization of the initially formed platinum alkyl complexes resulting from styrene insertion into a Pt–H bond to form either the primary phenethyl product (leading to normal or linear aldehyde) or the secondary α-methyl styryl product (leading to branched aldehyde).

The three chelating chiral diphosphine ligands chosen for this study, shown in Figure 1, are (+)-(2*S*,3*S*)-*O*-isopropylidene-2,3-dihydroxy-1,4-bis(diphenylphosphino)butane [DIOP], *N*-(*tert*-butoxycarbonyl)-(2*S*,4*S*)-4-(diphenylphosphino)-2-[(diphenylphosphino)methyl]pyrrolidine [BPPM], and the dibenzophosphole [DBP-BPPM] analogue. For the hydroformylation of styrene[3], DBP-BPPM gives an experimental b/n ratio greater than 3. DIOP and BPPM give experimental b/n ratios of 1.3 and 0.5, respectively. For comparison, the 1,2-bis[(diphenylphosphino)-methyl]cyclobutane [DPC] catalyst, observed to yield a b/n ratio of 1/99 for pentene, has been studied.[9]

The force field and benchmarks used are described in the Theoretical Details section, and the theoretical results are presented below in the Results and Discussion section.

Theoretical Details

The force field used is new to this work, and hence the functional forms and parameters developed must be validated by comparison with known structures. The functional forms and parameters used in the force field are presented in the Force Field subsection below. Minimizations were carried out on a set of 12 square-planar platinum(II) complexes chosen as being representative of the alkyl and acyl complexes relevant to a study of hydroformylation. The results are discussed in the Benchmark Results subsection.

Intermolecular (nonbonded) interactions are likely to dominate the selectivity of the interaction of a substrate with its binding site, particularly with respect to stereo- and regioselectivity. We assert below in the Results and Discussion section that π-stacking interactions are an important contributor to the observed regioselectivity. The ability of the present force field to energetically and geometrically describe this interaction must be validated. To this end, we have carried out molecular mechanics calculations on benzene dimer and crystalline benzene. The results are discussed in the Benzene subsection.

The molecules of interest have a large number of conformational degrees of freedom that are highly coupled; the ring portion of the chiral phosphine ligand is likely to move as a unit, and the phenyl rings of the phosphine are likely to move concertedly in a gear fashion. We use simulated annealing dynamics as our conformational searching tool. The overall procedure is provided in the Procedure subsection.

A. Force Field. The Dreiding force field[8] is extended in this work to include an atom type for square-planar platinum and an atom type for phosphorus coordinated to transition-metal centers. The parameters for the remaining atoms are taken directly from the published Dreiding force field. The individual terms in the force field are discussed below.

1. Bond Stretch. The bond stretching terms are of a harmonic form:

$$E_R = \tfrac{1}{2}k_{ij}(r - r_{ij})^2 \qquad (2)$$

where k_{ij}, the force constant ((kcal/mol)/Å^2), is assigned the value 700. The distance r_{ij} is the standard or natural bond length (Å); r_{ij} is assumed to be a sum of the atomic radii for atom types I and J (eq 3):

$$r_{ij} = r_i + r_j \qquad (3)$$

For platinum, a radius of 1.35 Å is used; for the new phosphorus atom type, a radius of 1.05 Å is used (the original Dreiding phosphorus atom type has a radius of 0.89 Å, a value appropriate for nucleic acids). These radii are used to determine the natural bond lengths, r_{ij}, for all bonds to platinum and bonds to coordinated phosphorus bonds, except bonds *between* platinum and the coordinated phosphorus. For this linkage, a coordinate-covalent bond, we use a platinum radius of 1.23 Å, resulting in a natural bond length between platinum and phosphorus of 2.28 Å.

2. Bond Bend. A harmonic in θ-expansion is employed to describe the angle bend term:

$$E_\theta = \tfrac{1}{2}K_{ijk}(\theta_{ijk} - \theta_0)^2 \qquad (4)$$

The natural angles are taken as being dependent only upon the nature of the central atom J. For platinum, a pair of natural square-planar angles of 90° and 180° are used with a force constant of 100 (kcal/mol)/rd^2 for each, and for the new phosphorus atom type a natural tetrahedral angle of 109.471° is used (in contrast, the original Dreiding phosphorus atom type has a natural angle of 93.3°, taken from PH_3).

3. Torsion. The torsional terms for two bonds IJ and KL connected via a common bond JK is chosen to be of the form

$$E_\phi = \tfrac{1}{2}V_\phi[1 + d\cos(n\phi)] \qquad (5)$$

where V_ϕ is one-half the rotational barrier (kcal/mol), n is the periodicity of the potential, and d (+1 or −1) is the phase factor. The rule-based scheme as outlined in the Dreiding paper is used for the new phosphorus atom type; torsional terms involving platinum as one of the central atoms J or K are not included.

4. Nonbonded Interaction. Nonbonded interactions (van der Waals forces) are included in the Dreiding force field, using a Lennard–Jones-type expression:

$$E_{vdw} = D_{ij}\{-2[x_{ij}/x]^6 + [x_{ij}/x]^{12}\} \qquad (6)$$

where D_{ij} is the well depth (kcal/mol) and x_{ij} is the van der Waals bond length (Å). Interactions are not calculated between atoms bonded to each other (1,2 interactions) or that are involved in angle interactions (1,3 interactions). The standard combination rules are assumed:

$$x_{ij} = \tfrac{1}{2}(RE_i + RE_j) \qquad D_{ij} = (DE_iDE_j)^{1/2} \qquad (7)$$

where RE is the atomic van der Waals distance (Å) and DE is the atomic van der Waals energy (kcal/mol). The van der Waals parameters for the new phosphorus atom type are taken from the Dreiding paper.[8] For platinum, we use RE = 2.97 and DE = 0.05.

(7) Halpern, J. In *Asymmetric Synthesis*; Morrison, J. D., Ed.; Academic Press: New York, 1985; Vol. 5, p 41.
(8) Mayo, S. L.; Olafson, B. D.; Goddard, W. A. *J. Phys. Chem.* **1990**, *26*, 8897.
(9) Kawabata, Y.; Hayashi, T.; Ogata, I. *J. Chem. Soc., Chem. Commun.* **1979**, 462.

Because there is a lack of structural data wherein van der Waals interactions at platinum dominate, the van der Waals parameters for platinum were taken directly from a determination of van der Waals parameters for the less ambigous case, silver. We believe this approximation is valid because of the polar coordinate-covalent nature of the bonding between platinum and the first coordination sphere ligands, and the insensitivity of non-nearest-neighbor distances to the precise van der Waals parameters used on platinum.

The van der Waals distance for silver ion was obtained by reproducing the experimental solid-state structures of the silver halides. The silver fluorides, chlorides, and bromides all crystalize in the cubic *Fm3m* space group, and hence the bonding interactions between silver and halide can be approximated as being ionic. The van der Waals distance RE was chosen to fit the unit cell parameter a = 5.556 Å[10] (space group *Fm3m*) for AgCl with an assigned well depth DE of 0.05 kcal/mol. The calculation was carried out with partial charges of +/–0.56 on Ag and Cl obtained from a QEq calculation[11] on the cubic tetramer. Van der Waals distances obtained for the other silver halides are in reasonable accord with the AgCl value if the partial charges are determined for each complex independently. The results are collected in supplementary material Table S.1.

5. Electrostatic Interactions. Electrostatic interactions are calculated by eq 8:

$$E_{el} = (332.0637)Q_iQ_j/\epsilon R_{ij} \qquad (8)$$

Q_i and Q_j are the partial charges in electron units, R_{ij} is the distance in angstroms, and ϵ is the dielectric constant. Interactions are not calculated between atoms bonded to each other (1,2 interactions) or that are involved in angle interactions (1,3 interactions). A dielectric constant of 1 is used in the current work. The partial charges are determined by using the recently developed QEq charge equilibration scheme.[11]

6. Comparison with Previous Pt Force Fields. Published platinum force fields have been used to study the binding interactions between Pt(II) and nitrogen donor ligands. In Hambley's work,[12] the only interactions involving the Pt were the Pt–N stretches. Pt–N bond distances of 2.01 and 2.03 Å were used for Pt–amine and Pt–purine bond distances, respectively. A Pt–N stretching force constant of 366 (kcal/mol)/Å^2 was reported. The values in the present work are 1.99 Å, 2.04 Å, and 700 (kcal/mol)/Å^2. Angle bend interactions about the Pt center are approximated as 1,3 nonbonded interactions involving the ligands; thus, electronic effects including angle-dependent rehybridization at Pt are ignored. Van der Waals and electrostatic terms at the metal center are also ignored. In our work, the charges at the Pt center ranged from +0.01 to +0.18 for the 12 benchmarks.

In the work of Lippard and co-workers,[13] both Pt–N stretch and N–Pt–N bend valence terms were included. A Pt–N distance of 2.00 Å was used with a force constant of 201 (kcal/mol)/Å^2. The N–Pt–N angle was set at 90° with a force constant of 42 (kcal/mol)/rd^2. Electrostatic interactions at platinum were included with the 2+ charge of the Pt(II) complex distributed between the Pt and the adjacent nitrogen ligands (a residual charge of +0.278 was placed on Pt). The van der Waals parameters used on Pt were not reported.

Miller et al. have[14a] modeled *cis*-Pt(II)–diammine binding to duplex DNA. A Pt–N distance of 1.996 Å with a force constant of 1346 (kcal/mol)/Å^2 was used. The Pt–N–H and the Pt–N–C angles were set at 109.5° and 120° with force constants of 80 and 300 (kcal/mol)/rd^2, respectively. A force constant of 500 (kcal/mol)/rd^2 was assigned to the N–Pt–N angle. A net charge of +1.2430 was placed on the platinum.

Landis and co-workers[14b] recently reported a new force field for square-planar complexes in general and have given specific force constants for platinum complexes derived from both a normal coordinate analysis and ab initio electronic structure calculations.

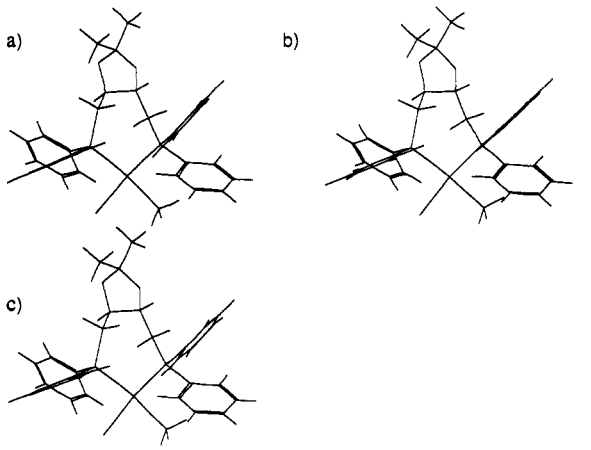

Figure 2. BEMGOP structures: (a) calculated structure with partial charges, (b) calculated structure without partial charges, (c) best calculated structure with partial charges from annealed dynamics.

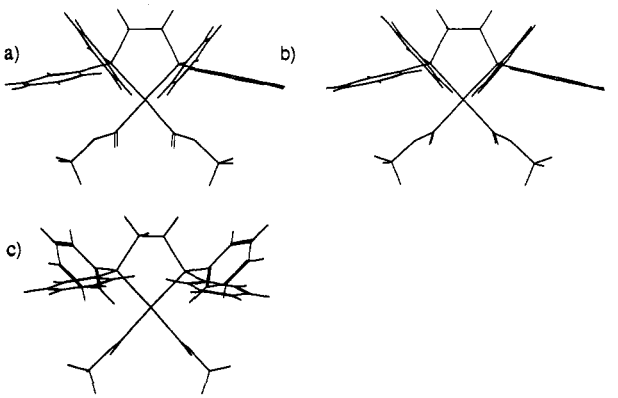

Figure 3. DAHXAL structures: (a) calculated structure with partial charges, (b) calculated structure without partial charges, (c) best calculated structure with partial charges from annealed dynamics.

B. Benchmark Results. Before presenting the results on our molecular mechanics study of the 12 Pt alkyl and acyl complexes, we wish to answer three additional questions: (1) Is there a local minimum near the experimental structure? (2) Can the force field withstand a simulated annealing conformational search procedure? (3) Does the addition/removal of partial charges, known to be important for "intermolecular" energetics, affect the isolated molecular structures?

These questions were probed with detailed calculations on two complexes, chloromethyl[(+)-(2*S*,3*S*)-*O*-isopropylidene-2,3-dihydroxy-1,4-bis(diphenylphosphino)butane]platinum(II) and [1,2-bis(diphenylphosphino)ethane-P,P']bis(methoxycarbonyl)-platinum(II). As shown in Figures 2 and 3, the initially minimized structures with and without partial charges, as well as the best structure from a five-cycle annealed dynamics calculation, are quite similar. For these two complexes, the force field is stable with respect to partial charges and simulated annealing.

The calculated and experimental Pt–X bond lengths and X–Pt–X bond angles for all 12 molecules studied are provided as supplementary material Table S.2. Note that the molecules were treated as isolated gas-phase species in the calculations. The first coordination sphere structural parameters are well reproduced; in general, the Pt–X bond distances are within 0.05 Å of experiment and the X–Pt–X bond angles within 4° of experiment. A

(10) *Crystal Data Determinative Tables*; Ondik, H. M., Wolten, G. M., Eds.; U. S. Department of Commerce, 1973; Vol. II.
(11) Rappé, A. K.; Goddard, W. A. *J. Phys. Chem.* **1991**, *95*, 3358.
(12) Hambley, T. W. *Inorg. Chim. Acta* **1987**, *137*, 15. Reily, M. D.; Hambley, T. W.; Marzilli, L. G. *J. Am. Chem. Soc.* **1988**, *110*, 2999. Hambley, T. W. *Inorg. Chem.* **1988**, *27*, 1073. Hambley, T. W. *J. Chem. Soc., Chem. Commun.* **1988**, 221.
(13) Kozelka, J.; Petsko, G. A.; Lippard, S. J.; Quigley, G. J. *J. Am. Chem. Soc.* **1985**, *107*, 4079. Kozelka, J.; Petsko, G. A.; Quigley, G. J.; Lippard, S. J. *Inorg. Chem.* **1986**, *25*, 1075. Kozelka, J.; Archer, S.; Petsko, G. A.; Lippard, S. J. Quigley, G. J. *Biopolymers* **1987**, *26*, 1245.
(14) a) McCarthy, S. L.; Hinde, R. J.; Miller, K. J.; Anderson, J. S.; Basch, H.; Krauss, M. *Biopolymers* **1990**, *29*, 823. b) Allured, V. S.; Kelly, C. M.; Landis, C. R. *J. Am. Chem. Soc.* **1991**, *113*, 1.

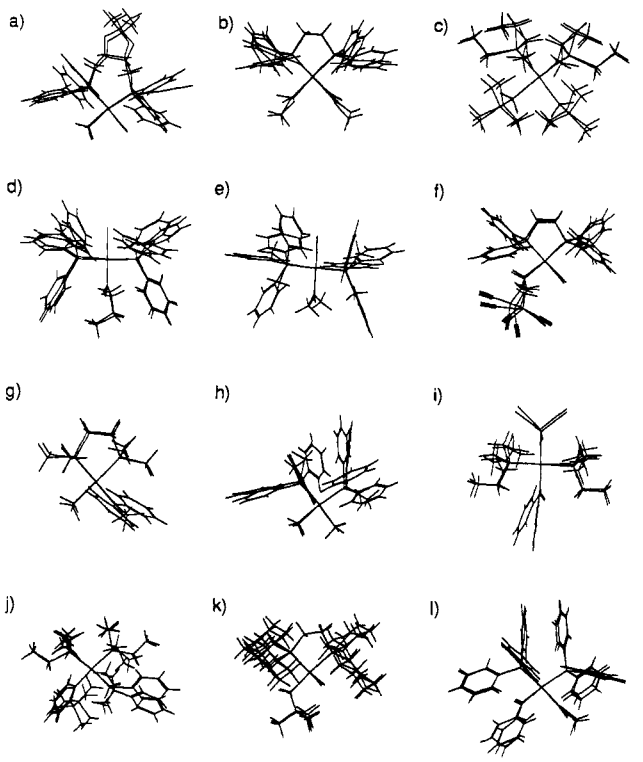

Figure 4. Superposition of the calculated (gas phase) and experimental (X-ray diffraction) benchmark structures.

detailed discussion of each structure is provided below.

1. Chloromethyl[(+)-(2*S*,3*S*)-*O*-isopropylidene-2,3-dihydroxy-1,4-bis(diphenylphosphino)butane]platinum(II).[15] The Pt–P distance trans to carbon is 0.02 Å short, but the Pt–P distance trans to chlorine is 0.07 Å too long (see Figure 4a). The fundamental or unstrained Pt–P bond distance presented above came from an examination of complexes containing cis phosphines with the phosphines trans to strong trans-effecting alkyl and acyl ligands. Given that a single fundamental Pt–P distance is used in the current force field, bonds to ligands *not* trans to strong trans-effecting ligands will be calculated to be too long—as observed here for the bond from Pt to P_2. The Pt–C bond distance is 0.04 Å short, and the Pt–Cl bond distance is 0.02 Å too long. All of the valence angles about Pt are within 2° of experiment except the Cl–Pt–C angle, which is 3° too large.

2. [1,2-Bis(diphenylphosphino)ethane-P,P′]bis(methoxycarbonyl)platinum(II).[16] The Pt–P bond distances are each 0.01 Å shorter than experiment (see Figure 4b). The Pt–C(carbonyl) bond distances are 0.02 Å short and 0.06 Å long. The C–Pt–C bond angle is 5° less than experiment. The C_1–Pt–P cis bond angle is 4° larger than experiment; the other C–Pt–P cis angle is 2° larger than experiment. The C_1–Pt–P trans angle is also 4° larger than experiment; the other C–Pt–P trans angle is 1° less than experiment. The dissymmetry in bond distances and angles is suggestive of significant crystal packing forces (vide infra).

3. Bis(neopentyl)bis(triethylphosphine)platinum(II).[17] The Pt–P bond distances are each 0.03 Å long, and the Pt–C are 0.04 Å long (see Figure 4c). The valence angles are within 2° of experiment except for the trans C–Pt–P angle, which is 4° smaller than experiment.

4. *n*-Butyrylchlorobis(triphenylphosphine)platinum(II).[18] The Pt–P distances are 0.02 Å too short. The Pt–C bond distance is 0.03 Å too long (see Figure 4d). The Pt–Cl bond distance is 0.10 Å too short, again reflecting the trans influence of an alkyl group not having been built into the force field for chlorine. One of the C–Pt–P bond angles is 3° too small; one of the Cl–Pt–P bond angles is also 3° too large. The remaining bond angles are within 2° of experiment.

5. *trans*-Acetylchlorobis(methyldiphenylphosphino)platinum-(II).[19] The Pt–P bond distances are in agreement with experiment, and the Pt–C bond distance is 0.01 Å too short (see Figure 4e). The Pt–Cl bond distance is 0.08 Å too short, reflective of a lack of a trans influence in the force field for the Pt–Cl bond. The two trans bond angles are 3° and 4° too small. The remaining angles are within 2° of experiment.

6. Chloro(3,3,4,4-tetracyanocyclopentyl)[bis(diphenylphosphino)ethylene-P,P′]platinum(II).[20] As above, the Pt–P bond trans to carbon is well described (0.01 Å too short), but the Pt–P bond trans to chlorine is 0.10 Å too long (see Figure 4f). The Pt–Cl is 0.01 Å too short, and the Pt–C distance is 0.01 Å too long. All of the valence angles about Pt are within 2° of experiment except the C–Pt–*cis*-P bond angle, which is 5° too large.

7. [1,2-Bis(dimethylphosphino)ethane-P,P′]methyl(methylphenylamino-N)platinum(II).[21] The Pt–P bond trans to carbon is 0.01 Å long; the Pt–P bond trans to nitrogen is 0.07 Å too long (see Figure 4g). The calculated Pt–C bond distance is 0.04 Å longer than experiment; the Pt–N bond distance is 0.08 Å shorter than experiment, and the Pt–P bond trans to nitrogen is 0.10 Å too long. All of the valence angles are within 2° of experiment except the trans bond angles (the N–Pt–P angle is 5° too large and the C–Pt–P angle is 3° too large).

8. *cis*-Dimethylbis(diphenylmethylphosphine)platinum(II).[22] The Pt–P bond distances are 0.03 Å too long, and the Pt–C bond distances are 0.01 Å too long (see Figure 4h). The C–Pt–C angle is 4° too large. One of the cis C–Pt–P angles is in error by 2°, but the other is in error by 4°. The P–Pt–P angle is 2° too small. One of the trans C–Pt–P angles is in error by 2°, the other by 4°. The molecule is observed to have a fairly significant tetrahedral distortion due to steric or crystal packing interactions. The calculated isolated molecule structure only partially reproduces this effect. The cis and trans C–Pt–C angles are nearly the same in the calculated structure. In the experimental structure, the cis C–Pt–P angles differ by 6°. The experimental trans C–Pt–P angles differ by 5°.

9. Benzoyl(trichlorotin)bis(triethylphosphine)platinum(II).[23] Both Pt–P bond distances are within 0.01 Å of experiment (see Figure 4i). The Pt–C bond distance is in agreement with experiment. The Pt–Sn bond distance is 0.12 Å too long. This bond is trans to carbon; as such, it should be calculated to be too short (due to the lack of a trans influence in the force field). The Dreiding Sn distance parameter is probably inappropriate for describing Sn in this valence environment. The trans P–Pt–P and C–Pt–Sn angles are calculated to be too large by 3° and 5°, respectively. The cis bond angles are all within 1° of experiment.

10. (2-*tert*-Butylphenyl)(2-methyl-2-phenylpropyl)bis(triethylphosphine)platinum(II).[24] The Pt–P bond distances are 0.02 and 0.03 Å too long (see Figure 4j). The aryl–Pt bond distance is 0.01 Å too long, and the alkyl–Pt bond distance is 0.03 Å too long. All of the Pt valence angles are within 2° of experiment.

11. *cis*-Hydridoneopentyl[1,2-bis(dicyclohexylphosphino)-ethane-P,P′]platinum(II).[25] The Pt–P bond distances trans to carbon and hydrogen are 0.03 and 0.02 Å too long, respectively (see Figure 4k). The Pt–C bond distance is in agreement with

(15) Payne, N. C.; Stephan, D. W. *J. Organomet. Chem.* **1982**, *228*, 203.
(16) Bryndza, H. E.; Kretchmar, S. A.; Tulip, T. H. *J. Chem. Soc., Chem. Commun.* **1985**, 977.
(17) Ibers, J. A.; DiCosimo, R.; Whitesides, G. M. *Organometallics* **1982**, *1*, 13.
(18) Bardi, R.; Piazzesi, A. M.; Cavinato, G.; Cavoli, P.; Toniolo, L. *J. Organomet. Chem.* **1982**, *224*, 407.
(19) Bennett, M. A.; Ho, K.-C.; Jeffery, J. C.; McLaughlin, G. M.; Robertson, G. B. *Aust. J. Chem.* **1982**, *35*, 1311.
(20) Calligaris, M.; Carturan, G.; Nardin, G.; Scrivanti, A.; Wojcicki, A. *Organometallics* **1983**, *2*, 865.
(21) Bryndza, H. E.; Fultz, W. C.; Tam, W. *Organometallics* **1985**, *4*, 939.
(22) Wisner, J. M.; Bartczak, T. J.; Ibers, J. A. *Organometallics* **1986**, *5*, 2044.
(23) Albinati, A.; von Gunten, U.; Pregosin, P. S.; Ruegg, H. J. *J. Organomet. Chem.* **1985**, *295*, 239.
(24) Griffiths, D. C.; Joy, L. G.; Skapski, A. C.; Wilkes, D. J.; Young, G. B. *Organometallics* **1986**, *5*, 1744.
(25) Hackett, M.; Ibers, J. A.; Jernakoff, P.; Whitesides, G. M. *J. Am. Chem. Soc.* **1986**, *108*, 8094. Hackett, M.; Ibers, J. A.; Whitesides, G. M. *J. Am. Chem. Soc.* **1988**, *110*, 1436.

Table I. Results of Crystal Minimization (Distances (Å), Angles (deg))

	ClMe(DIOP)Pt-(II)		$(MeOCO)_2$-(DPPE)Pt(II)	
parameter	calcd	X-ray	calcd	X-ray
$Pt-P_1$	2.32	2.32	2.29	2.29
$Pt-P_2$	2.30	2.23	2.30	2.30
$Pt-C_1$	2.13	2.17	2.04	2.06
$Ptt-Cl(C_2)$	2.35	2.32	2.05	2.06
P_1-Pt-P_2	98	99	86	85
$C_1-Pt-Cl(C_2)$	84	82	83	90
C_1-Pt-P_1	169	168	94	90
C_1-Pt-P_2	90	92	177	175
$Cl(C_2)-Pt-P_1$	89	87	173	177
$Cl(C_2)-Pt-P_2$	171	174	97	94

experiment. The Pt–H bond distance is 0.11 Å too long. However, X-ray diffraction X–H bond distances are known to be systematically at least 0.1 Å too short because the diffraction experiment samples electron density rather than nuclear position. All of the valence angles except two are within 2°. The H–Pt–*cis*-P angle is 9° too small, and the C–Pt–H angle is 7° too large.

12. *cis*-Benzoyl(methoxycarbonyl)bis(triphenylphosphine)-platinum(II).[26] The Pt–P bond distance trans to the benzoyl ligand is calculated to be 0.04 Å too short (see Figure 4l). The Pt–P bond distance trans to the methoylcarbonyl ligand is in agreement with experiment. The Pt–benzoyl distance is in agreement with experiment, and the methoxycarbonyl–Pt distance is 0.03 Å too long. All of the valence angles are within 3° of experiment.

As is evident from the superimposed experimental and calculated structures collected in Figure 4, there are substantial deviations in the tertiary structures. These deviations can logically be attributed to crystal packing forces not included in the isolated molecule calculations. This hypothesis was tested by carrying out minimizations on chloromethyl[(+)-(2*S*,3*S*)-*O*-isopropylidene-2,3-dihydroxy-1,4-bis(diphenylphosphino)butane]platinum(II) and [1,2-bis(diphenylphosphino)ethane-P,P']bis(methoxycarbonyl)-platinum(II) in a crystal environment. The calculated and experimental valence parameters are collected in Table I.

Chloromethyl[(+)-(2*S*,3*S*)-*O*-isopropylidene-2,3-dihydroxy-1,4-bis(diphenylphosphino)butane]platinum(II). The Pt–P distance trans to carbon is now in agreement with experiment, but the Pt–P distance trans to chlorine is still 0.07 Å too long. The Pt–C bond distance is still 0.04 Å short, and the Pt–Cl bond distance is 0.03 Å too long. The valence angles are now within 3° of experiment.

[1,2-Bis(diphenylphosphino)ethane-P,P']bis(methoxycarbonyl)platinum(II). The Pt–P bond distances are now in agreement with experiment. The Pt–C(carbonyl) bond distances are now 0.01 and 0.02 Å short of experiment—compared to errors of –0.02 and +0.06 Å for the isolated molecule calculation. The C–Pt–C bond angle is now 7° less than experiment (it was 5° less than experiment for the isolated molecule minimization). One of the C_1–Pt–P cis bond angles is 4° larger than experiment; the other 3° larger than experiment. One of the C_1–Pt–P trans angles is 3° smaller than experiment; the other is 2° larger than experiment.

The agreement between calculated and experimental tertiary structure is increased significantly when the metal complex is placed in a crystal environment (see Figure 5). This improvement in structural reproduction is evident from a comparison of Figure 4a with 5a and 4b with 5b. In Figure 4a,b, the isolated molecule calculated and experimental structures for chloromethyl[(+)-(2*S*,3*S*)-*O*-isopropylidene-2,3-dihydroxy-1,4-bis(diphenylphosphino)butane]platinum(II) and [1,2-bis(diphenylphosphino)ethane-P,P']bis(methoxycarbonyl)platinum(II) are superimposed. In Figure 5a,b, the corresponding superposition of crystal structures is presented. The importance of crystal packing forces is dramatic and is reproduced in the crystal calculation.

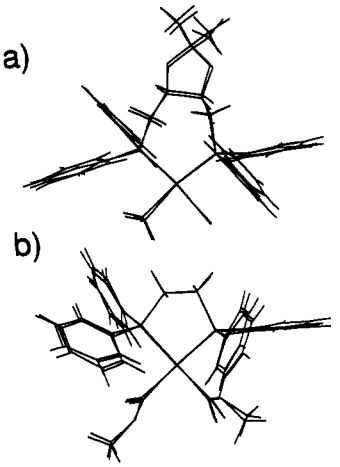

Figure 5. Superposition of the calculated (crystal) and experimental (X-ray diffraction) structures for chloromethyl[(+)-(2*S*,3*S*)-*O*-isopropylidene-2,3-dihydroxy-1,4-bis(diphenylphosphino)butane]platinum-(II) and [1,2-bis(diphenylphosphino)ethane-P,P')bis(methoxycarbonyl)-platinum(II).

C. Benzene. A major conclusion of the present work is the importance of an attractive nonbonded interaction between a pair of aromatic π-rings. The interaction between π-rings has been the subject of a number of theoretical studies on benzene ranging from the solid-state structure,[27,28] to the liquid-state structure,[29] to the interaction of a pair of molecules in the gas phase.[30] In addition, the importance of π-stacking interactions in organic chemistry has been discussed.[31] The carbon and hydrogen van der Waals parameters used are likely to be sufficient for the present study because the parameters from the Dreiding paper[8] are a derivative of those developed by Williams.[27] Williams' parameters were developed for reproducing the solid-state structures and energies of sublimation for a set of organic molecules that included benzene. In Williams' work, as in the present work, the intermolecular interactions were described in terms of van der Waals and partial charge electrostatics. The charges on carbon and hydrogen were fixed by Williams and Starr at –0.15 and +0.15, respectively. Using the current Qeq methodology,[11] we obtain partial charges of –0.10 and +0.10, respectively, for an isolated benzene molecule.

To test the adequacy of the present force field for intermolecular π–π-interactions, calculations were carried out on a crystal of benzene. The agreement with experimental lattice constants[32] is good (errors in *a*, *b*, and *c* of 0.07, 0.11, and 0.07 Å, respectively [calculated values 7.39, 9.58, 6.96 Å; experimental values 7.46, 9.67, 7.03 Å]). Williams and Starr[27] obtained errors of 0.06, 0.18, and 0.41 Å, for *a*, *b*, and *c*, respectively. Allinger and Lii[28] reported errors of 0.28, 0.15, and 0.04 Å, for *a*, *b*, and *c*, respectively. The Dreiding force field energy of sublimation of 11.3 kcal/mol is in error by 0.9 kcal/mol (experimental value 10.4 kcal/mol). Williams and Starr[27] and Allinger and Lii[28] reported energies of sublimation of 10.4 and 10.3 kcal/mol, respectively.

(26) Sen, A.; Chen, J.-T.; Vetter, W. M.; Whittle, R. R. *J. Am. Chem. Soc.* **1987**, *109*, 148.

(27) Williams, D. E. *Acta Crystallogr.* **1974**, *A30*, 71. Williams, D. W.; Starr, T. L. *J. Comput. Chem.* **1977**, *1*, 173.

(28) Allinger, N. L.; Lii, J.-H. *J. Comput. Chem.* **1987**, *8*, 1146.

(29) Jorgensen, W. L.; Severance, D. L. *J. Am. Chem. Soc.* **1990**, *112*, 4768.

(30) Law, K. S.; Schauer, M.; Bernstein, E. R. *J. Chem. Phys.* **1984**, *81*, 4871. Schauer, M.; Bernstein, E. R. *J. Chem. Phys.* **1985**, *82*, 3722.

(31) Trost, B. M.; O'Krongly, D.; Belletire, J. L. *J. Am. Chem. Soc.* **1980**, *102*, 7595. Ciliberto, E.; Doris, K. A.; Pietro, W. J.; Reisner, G. M.; Ellis, D. E.; Fragala, I.; Herbstein F. H.; Ratner, M. A.; Marks, T. J. *J. Am. Chem. Soc.* **1984**, *106*, 7748. Kamiichi, K.; Danshita, M.; Minamino, N.; Doi, M.; Ishida, T.; Inoue, M. *FEBS Lett.* **1986**, *195*, 57. Ishida, T.; Doi, M.; Ueda, H.; Inoue, M.; Scheldrick G. M. *J. Am. Chem. Soc.* **1988**, *110*, 2286. Tucker, J. A.; Houk, K. N.; Trost, B. M. *J. Am. Chem. Soc.* **1990**, *112*, 5465. Huner, C. A.; Sander, J. K. M. *J. Am. Chem. Soc.* **1990**, *112*, 5525.

(32) Cox, E. G.; Cruickshank, D. W. J.; Smith, J. A. S. *Proc. R. Soc. London* **1958**, *A247*, 1. Bacon, G. E.; Curry, N. A.; Wilson, S. A. *Proc. R. Soc. London* **1964**, *A279*, 98.

For a pair of isolated benzene molecules, Jorgenson and Severence[29] calculated the perpendicular conformation to be bound by 2.3 kcal/mol, and the π-stacked conformation to be bound by 2.1 kcal/mol. Allinger and Lii[28] calculated both conformations to be bound by 1.7 kcal/mol. We calculate the perpendicular conformation to be bound by 2.3 kcal/mol, and the π-stacked conformation to be bound by 3.1 kcal/mol. The experimental binding energy is still in question, though an upper bound of 2.8 kcal/mol can be reasonably assumed.[33] The available experimental evidence is not sufficient to distinguish between the perpendicular and π-stacked conformations,[29,32] perhaps due to the inherent softness of the potential energy surface. Conservatively, we estimate that the molecular mechanics derived energy of the π-stacking interaction in the Pt complexes is too large by approximately 2 kcal/mol.

D. Procedure. All of the reported calculations were carried out by using the Biograf and Polygraf molecular simulation programs,[34] version 2.1. The Biograf and Polygraf energy and first-derivative terms used were verified by comparison of results obtained with a set of independently developed in-house codes.[35] The first and second derivatives of the in-house codes have further been numerically verified via numerical first and second differences using 128-bit arithmetic on a Micro Vax II. These comparisons have been made for isolated molecules as well as crystalline systems including Ewald sums.

In order to address the large number of conformational degrees of freedom available in the complexes studied, the minimized charge equilibrated trial structure for each complex discussed in the Results and Discussion section below was subjected to 5–10 cycles of annealed dynamics from 0 to 600 K with a symmetric temperature ramp of 1°/1 fs. Each structure from the resulting collection of structures was minimized by using a Fletcher–Powell minimization procedure, and the charges were reequilibrated.

The isolated molecule minimizations for the suite of benchmark molecules used the crystal coordinates for one of the molecules within the unit cell obtained from the Cambridge Data Bank[36] as the trial guess. The minimization proceeded until the convergence criteria of a residual rms force of 0.1 (kcal/mol)/Å was achieved. The partial charges were calculated for the experimental solid-state structure.

The solid-state molecular mechanics minimizations used the crystal coordinates and cell parameters obtained from the Cambridge Data Bank[36] as the trial guess. For chloromethyl[(+)-(2*S*,3*S*)-*O*-isopropylidene-2,3-dihydroxy-1,4-bis(diphenylphosphino)butane]platinum(II), the unit cell consists of four molecules. For [1,2-bis(diphenylphosphino)ethane-P,P′]bis(methoxycarbonyl)platinum(II), the unit cell consists of two molecules. Electrostatic interactions were summed over a 5 × 5 × 5 grid in real space and then continued periodically with Ewald sums. During minimization, the coordinates of the four (chloromethyl[(+)-(2*S*,3*S*)-*O*-isopropylidene-2,3-dihydroxy-1,4-bis(diphenylphosphino)butane]platinum(II)) or two [1,2-bis(diphenylphosphino)ethane-P,P′]bis(methoxycarbonyl)platinum(II)) molecules in the unit cell as well as the unit cell coordinates were optimized.

To minimize errors in the theoretical methodology used, we calculated the energetics for a pair of isodesmic reactions[37] (eqs 9 and 10) for the branched and normal Pt alkyl intermediates, respectively. The energetics found from eqs 9 and 10 are used to assess the relative stabilizing interactions between the aryl ligand and the chelating phosphine. The annealed dynamics calculations with $SnCl_3^-$ present were carried out with the tin anion not bound to the platinum. The anion was placed in several different starting geometries. The starting complexes were minimized, and the charges were equilibrated over the whole platinum–tin complex. Five cycles of annealed dynamics were then run from 0 to 400 K, the resulting set of structures were reminimized by using the Fletcher–Powell method, and the charges were requilibrated. In the benzene droplet calculation, a tetragonal sovent cage was built around the platinum complex with a grid space of 5 Å, an inner cutoff of 5 Å, and an outer cutoff of 10 Å. The outer layers of benzene were removed, leaving 20 benzene molecules in the solvent shell. The solvated complex was minimized by using the Fletcher–Powell method and then subjected to five cycles of annealed dynamics with a temperature range of 0–300 K. The resulting set of structures were then reminimized.

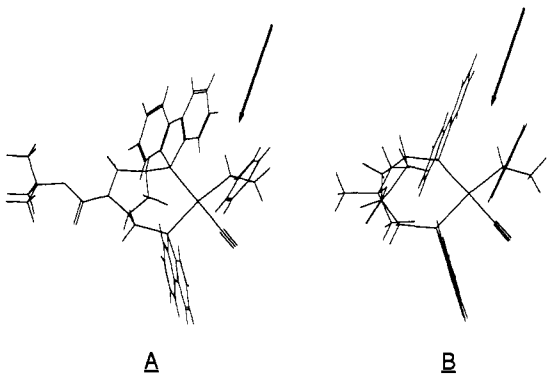

Figure 6. Molecular mechanics structures for the DBP-BPPM phenethyl (A) and α-methyl styryl (B) complexes. The arrows indicates the location or absence of the π-stacking interaction.

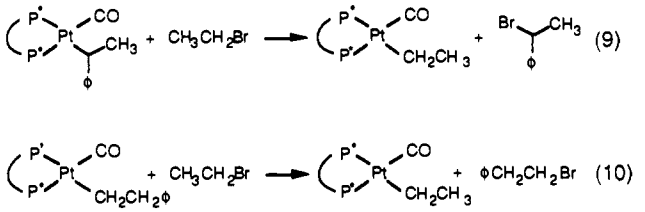

Results and Discussion

The present computational study has focused on the differential stabilization of the branched and normal alkyls formed through an olefin insertion into a Pt–H bond. As discussed in the Theoretical Details section, the isodesmic reactions (eqs 9 and 10) form the basis for our numerical comparison. For the DBP-BPPM phosphine Pt complex, we find a significant stabilization of the α-methyl styryl substituent (the reaction in eq 9). The α-methyl styryl complex is prefentially stabilized by 1–1.5 kcal/mol. When the energetics for the reactions in eqs 9 and 10 are compared for DBP-BPPM, we find that the branched, α-methyl styryl product is preferred over the normal, phenethyl product by 3 kcal/mol. For BPPM, the reverse preference is found: the normal, phenethyl product is preferred by 3 kcal/mol. The net 6 kcal/mol differential found for the two prior olefin insertion equilibria in eq 1 is consistent with, though significantly larger than, the energetics associated with the experimental b/n ratios of 0.5 and 3 for BPPM and DBP-BPPM, respectively. The BPPM catalyst preferentially forms the normal aldehyde product, whereas DBP-BPPM forms the branched aldehyde product.

The regiochemistry of the DBP-BPPM catalyst can be explained by proposing a favorable interaction between the phenyl ring of the alkyl ligand and the dibenzophosphole substituent of the phosphine. The presence or absence of these nonbonded inter-

(33) Nishiyama, I.; Hanazaki, I. *Chem. Phys. Lett.* **1985**, *117*, 99. Johnson, R. D.; Burdenski, S.; Hoffbauer, M. A.; Giese, C. F.; Gentry, W. R. *J. Chem. Phys.* **1986**, *84*, 2624. Grover, J. R.; Walter, E. A.; Hui, E. T. *J. Phys. Chem.* **1987**, *91*, 3233. Lin, S. H.; Selzle, H. L.; Bornsen, K. O.; Schlag, E. W. *J. Phys. Chem.* **1988**, *92*, 1469, Kiermeier, A.; Ernstberger, B.; Neusser, H. J.; Schlag, E. W. *J. Phys. Chem.* **1988**, *92*, 3785. Grover, J. R.; Walters, E. A.; Baumgartel, H. *J. Phys. Chem.* **1989**, *93*, 7534. Selzle, H. L.; Neusser, H. J.; Ernstberger, B.; Krause, H.; Schlag, E. W. *J. Phys. Chem.* **1989**, *93*, 7535.

(34) Biograf and Polygraf obtained from the BioDesign subsidiary of Molecular Simulations Inc., 199 S. Los Robles Avenue, Suite 540, Pasadena, CA 91101.

(35) Skiff, W. M.; Ramachandran, S.; Lenz, T. J.; Rappé, A. K. Unpublished results.

(36) Kennard, O. Cambridge Crystallographic Data Centre, University Chemical Laboratory, Lensfield Road, Cambridge, CBZ 1 EW, UK.

(37) Hebre, W. J. *Acc. Chem. Res.* **1976**, *9*, 399.

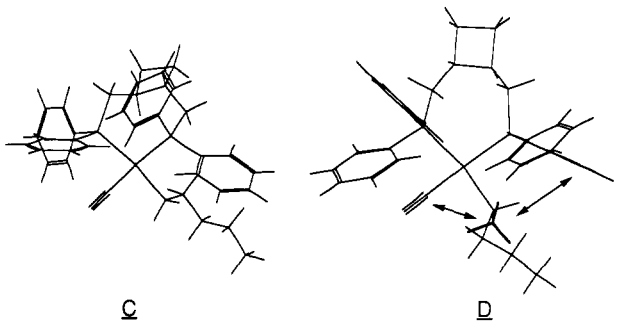

Figure 7. Molecular mechanics structure for the normal pentenyl (C) and α-methyl butyl (D) DPC complexes. The arrows indicate the location of the unfavorable steric interactions.

actions can be visually observed in the molecular mechanics derived structures of the complexes. The structures for the DBP-BPPM phenethyl (A) and α-methyl styryl (B) complexes are shown in Figure 6. The arrows indicate the lack (A) and occurance (B) of a π-stacking interaction.

To further probe the energetic factors contributing to the regioselectivity, calculations were carried out for the branched and normal DPC Pt complexes resulting from reaction with 1-pentene. The catalyst containing this phosphine is known to give a b/n ratio of 1/99.[9] We find the normal isomer to be more stable than the branched isomer by 7 kcal/mol, in agreement with experiment. The source of this differential stabilization can be seen visually in Figure 7. Here the phosphine ligand undergoes a significant distortion in going from the normal alkyl conformation, C, to the α-methyl conformation, D. This distortion occurs to minimize competing unfavorable steric interactions between the α-methyl group and the coordinated carbon monoxide, and between the α-methyl group and the phenyl group of the adjacent phosphine. When the pentyl calculations were repeated for the DBP-BPPM chelating phosphine complex, the normal isomer was found to be favored by 5 kcal/mol over the branched isomer due to similar interactions.

For the chiral complexes studied, the α-methyl styryl complexes are calculated to have a significant π-stacking interaction between the phenyl ring of the aryl ligand and the aryl substituent of the phosphine ligand. In contrast, phenethyl ligands do not exhibit a significant π-interaction with the aryl substituent of the phosphine ligand. The increased alkyl chain length effectively prevents the aryl substituent of the phenethyl ligand from interacting with an aryl substituent of the chiral phosphine ligand. For DBP-BPPM, this favorable "steric" interaction is sufficient to overcome the steric repulsion between the methyl of the α-methyl styryl and the adjacent carbonyl in the complex. This steric repulsion between the methyl of the branched alkyl and the adjacent carbonyl in the complex dominates for the BPPM complexes as well as for the pentenyl case discussed above, thus resulting in a preference for the normal complex.

Experimentally, hydroformylation reactions are run in benzene solvent.[3] To probe the effect of benzene solvent on the π-stacking interaction, the minimization/annealed dynamics procedure was applied to the branched DBP-BPPM complex in a benzene droplet. The π-stacking interaction was partially disrupted, as shown in Figure 8. Though determination of the energetic consequence of this partial disruption would require simulation in a liquid rather than a droplet, it is reasonable to conclude that experimental choice of solvent is likely to affect the degree of π-stacking and therefore the regiochemistry. Further, it is reasonable to conclude that the computational overestimation of the b/n ratio is in part due to the lack of a solvent being present in the current simulations.

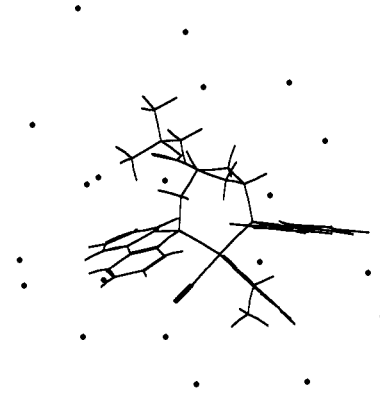

Figure 8. Molecular mechanics structure for α-methyl styryl DBP-BPPM in a benzene droplet.

Experimentally, the Pt complex used is either preformed as $L_2Pt(Cl)SnCl_3$ or is formed in situ by combining L_2PtCl_2 with $SnCl_2$. In either case, the $SnCl_3^-$ anion is thought to play an important role in the overall catalytic activity. In order to test the dependence of the π-stacking interaction on the model complex chosen, the calculational procedure was carried out for the DBP-BPPM Pt α-methyl styryl carbonyl complex with $SnCl_3^-$ present as a counterion. The lowest energy conformers retained the π-stacking interaction.

Summary and Conclusions

This work presents results using the Dreiding force field, augmented to include square-planar Pt and a new P atom type. The experimental first coordination sphere geometries of a series of phosphine-ligated square-planar Pt acyls and alkyls were well reproduced in isolated single-molecule calculations. The tertiary structures were reproduced by carrying out minimizations in a crystal environment. The Pt force field was further applied to an investigation of the origin of the regioselectivity in the Pt-catalyzed hydroformylation reaction. The factors favoring primary versus secondary alkyl intermediate formation, resulting from pentene and styrene insertion into a Pt–H bond, were investigated. We find steric interactions determine the regiochemistry of the pentene insertion: A dramatic phosphine ligand distortion occurs in the α-methyl intermediate due to competing steric interactions between the α-methyl group and the coordinated carbon monoxide, and between the α-methyl group and the phenyl group of the adjacent phosphine. This distortion destabilizes the branched intermediate relative to the normal intermediate, predicting a low b/n ratio in the resulting aldehydes, in agreement with experiment. A favorable π-stacking interaction between the phenyl ring of the α-methyl styryl and a dibenzophosphole substituent of the phosphine was discovered to be important in the DBP-BPPM intermediate. We conclude that π-stacking should be considered as a factor in organometallic reactions involving aryl olefins and ligands containing aryl substituents.

Acknowledgment. We thank BioDesign for the use of the Biograf and Polygraf molecular simulation programs. This research was partially supported by a grant (GM39038) from the National Institutes of Health.

Supplementary Material Available: Tables listing van der Waals distance optimization and discrete molecule minimization results (4 pages). Ordering information is given on any current masthead page.